

# Peristaltic flow in non-uniform vessels of the micro-circulatory system

S. Maiti<sup>1</sup>‡ and J.C.Misra<sup>2</sup>§

<sup>1</sup> School of Medical Science and Technology & Center for Theoretical Studies, IIT, Kharagpur-721302, India

<sup>2</sup> Professor of Applied of Mathematics, Indian Institute of Technology, Patna-800013, India

**Abstract.** Of concern in the paper is generalized a theoretical study concerning the peristaltic flow of blood in the micro-circulatory system. The vessel is considered to be of non-uniform cross-section and blood to be a non-Newtonian fluid. The progressive wave front of the peristaltic flow is supposed sinusoidal/straight section dominated (SSD) (expansion/contraction type); Reynolds number is considered to be small with reference to the flow of physiological fluids. The non-Newtonian behaviour of blood is illustrated by considering the Herschel-Bulkley fluid model. The objective of the study has been to examine the effect of the effects of amplitude ratio, mean pressure gradient, yield stress and the power law index on the velocity distribution, wall shear stress, streamline pattern and trapping. Considerable quantitative differences between the results obtained for transport in two dimensional channel and an axisymmetric circular tube are noticed. The study shows that peristaltic pumping, flow velocity and wall shear stress are significantly affected by the non-uniform geometry of blood vessels. Moreover, the magnitude of the amplitude ratio and the value of the fluid index are important parameters that affect the flow behaviour. The novel feature due to SSD wave on said flow behaviour has also been discussed.

*Keywords:* *Non-Newtonian Fluid, Flow Reversal, Wall Shear Stress, Trapping, SSD Wave.*

‡ somnathm@cts.iitkgp.ernet.in (S.Maiti)

§ misrajc@rediffmail.com (J.C.Misra)

## 1. Introduction

Peristaltic transport through different vessels of physiological systems by means of peristaltic waves is well known to physiologists as a natural mechanism of pumping materials in the case of most physiological fluids. Apart from physiological studies, many of the essential fluid mechanical characteristics of peristalsis have also been elucidated in different engineering analyses carried out by different researchers. Such types of characteristics usually occur when the flow is induced by a progressive wave of area contraction/expansion along the length of the boundary of a fluid-filled distensible tube. Benefits that can be derived from regarding the studies on peristaltic movement are available in our earlier communications (Misra and Pandey 1994, 1995, 1999, 2001a, 2001b, 2002, Misra *et al* 2008, maiti and misra 2011) and also in other references e.g., Guyton and Hall (2006), Jaffrin and Shapiro (1971).

### Nomenclature

$b$	Wave amplitude
$a_0$	Radius of the tube at the inlet
$H$	Displacement of the wall in the radial direction
$k$	Reciprocal of $n$
$k_1$	A parametric constant
$n$	Flow index number
$P$	Fluid pressure
$Q$	Flux at axial location
$t_1$	Time
$R, \theta, Z$	Cylindrical co-ordinates
$U, V, W$	Velocity components in $Z, R, \theta$ directions respectively
$\delta$	Wave number
$\Delta p$	Pressure difference between ends of the tube
$\lambda$	Wave length of the travelling wave motion at the wall
$\mu$	Blood viscosity
$\nu$	Kinematic viscosity of blood
$\phi$	Amplitude ratio
$\rho$	Density of blood
$\tau_0$	Yield stress of blood
$\tau_h$	Wall shear stress

The phenomenon of peristalsis has quite important applications in the design and construction of many useful devices of biomedical engineering and technology, artificial blood devices such as heart-lung machine, blood pump machine, dialysis machine etc. A theoretical foundation of peristaltic transport primarily with inertia-free Newtonian flows driven by sinusoidal transverse waves of small amplitude was suggested by Fung and Yih (1968). Shapiro *et al* (1969) first presented the closed form solutions for an infinite train of peristaltic waves for small Reynolds number flow, where the wave length is long but of arbitrary wave amplitude. The

said investigations (Fung and Yih 1968, Shapiro *et al* 1969) witnessed a variety of important applications that have been proved to be quite useful in elucidating the functioning of various physiological systems, such as flows in the ureter, the gastro-intestinal tract, the small blood vessels of the micro-circulatory system and other glandular ducts. Conditions for the existence of physiologically significant phenomena of trapping and reflux in peristaltic transport were also determined by Shapiro *et al* (1969). Some of the references to earlier literatures on peristaltic flow of physiological fluids are available in (Jaffrin and Shapiro 1971, Srivastava and Srivastava 1984), while brief reviews of relatively recent literatures can be found in (Tsiklauri and Beresnev 2001, Mishra and Rao 2005, Yaniv *et al* 2009, Jimenez-Lozano *et al* 2009). Several other studies concerned with the analysis of different problems of peristaltic transport of various physiological fluids were reported by different investigators (Usha and Rao 1995, Takabatake and Ayukawa 1982, Jimenez-Lozano and Sen 2010, Bohme and Friedrich 1983, Srivastava and Srivastava 1985, Provost and Schwarz 1994, Chakraborty 2006). Past experimental observations indicate that the non-Newtonian behaviour of whole blood mainly owes its origin to the presence of erythrocytes. As early as in the sixth decade of the last century, different groups of scientists (Rand *et al* 1964, Bugliarello *et al* 1965, Chien *et al* 1965) made an observation that the non-Newtonian character of blood is prominent as soon as the hematocrit rises above 20%. However, it plays a dominant role, when hematocrit level lies between 40% and 70%.

It is known that the nature of blood flow in small vessels (radius  $< 0.1$  mm) and at low shear rate ( $< 20 \text{ sec}^{-1}$ ) can be represented by a power law fluid (Charm and Kurland 1965, 1974). As reported by Merrill *et al* (1965), Casson model seems to be satisfactory for blood flowing in tubes of  $130\text{-}1000\mu$ . Scott Blair and Spanner (1974) estimated that blood obeys Casson model for moderate shear rate flows. However, they did not report any difference between Casson and Herschel-Bulkley plots over the range where Casson plot is valid for blood. They observed that for cow's blood, Herschel-Bulkley model is more appropriate than Casson model has been found by them. The results presented in the sequel for shear thinning and shear thickening fluids are quite relevant for the study of blood rheology. It is important to mention here that normal blood usually behaves like a shear thinning fluid for which with the increase in shear rate, the viscosity decreases. As mentioned in (Fung 1981, White 1974, Xue 2005) in the case of hardened red blood cell suspensions, the fluid behaviour is that of a shear thickening fluid for which with the fluid viscosity is enhanced due to an elevation of the shear rate.

It is well-known that physiological vessels are usually non-uniform (Wiedman 1963, Wiederhielm 1967, Lee and Fung 1971). Some initial attempts to perform theoretical studies pertaining to peristaltic transport of physiological fluids in vessels of non-uniform cross section were made in several researchers (Srivastava and Srivastava 1984, Wiederhielm 1967, Lee and Fung 1971, Gupta and Seshadri 1976, Srivastava and Srivastava 1983). In all these studies, the physiological fluids were considered either as Newtonian fluids or non-Newtonian fluids described as Casson/power-law fluids. However, the different flow characteristics have not been adequately explained in these studies. Herschel-Bulkley models are of course, more suitable to represent physiological fluids, because the fluids represented by this model describe very well material

flows with a non-linear stress relationship depicting the behaviour of shear-thinning/shear-thickening fluids that are of much importance in the field of biomedical engineering (Malek *et al* 2002). Among the various types of non-Newtonian models used to represent physiological fluids, Herschel-Bulkley fluid model is more general. Use of this model has the advantage that results for fluids represented by Bingham plastic model, power law model, Newtonian fluid model can be derived from those of the Herschel-Bulkley fluid model. Also Herschel-Bulkley fluid model is found to yield more accurate results than many other non-Newtonian models.

In the consideration of all the above, a study concerning the peristaltic flow of blood in a non-uniform vessel of micro-circulatory system has been undertaken here, by treating blood as a non-Newtonian fluid. It is worthwhile to mention that although flow through axisymmetric tubes is qualitatively almost similar to the case of flow in channels, magnitude of different physiological quantities associated with flow and pressure differ appreciably differ by one another. The mathematical analysis presented here is particularly suitable for investigating the peristaltic motion of blood through vessels in micro-vessels, e.g. arterioles and venules. Since for blood flow in the micro-circulatory system, the Reynolds number is low and since the ratio between radius of the tube and the wave length is small, the theoretical analysis of the problem under consideration has been performed by using the lubrication theory (Shapiro *et al* 1969). Basing upon the study, extensive numerical calculations have been made with the help of derived analytical expressions. Keeping a specific situation of micro-circulation in view, with the purpose of examining the pumping performance, the computational results are presented for the velocity distribution of blood, wall shear stress distribution as well as the streamline pattern and trapping. Influence of SSD wave front on various flow behaviour of peristaltic movement has also been discussed. The plots give a clear view of the qualitative variation of various fluid mechanical parameters.

The analysis bears a strong promise of some important applications by which we can have a better insight of the micro-circulatory system. The analysis has an important bearing on the clinical procedure of extra-corporeal circulation of blood through the use of the heart-lung machine that may result in damage of erythrocytes owing to high variation of the wall shear stress. In addition, the results should useful application in the development of roller pumps and arthro pumps by which fluids are transported in living organs.

## 2. Formulation

Peristaltic motion of blood in arterioles and venules will be studied here, by considering blood as an incompressible viscous non-Newtonian fluid. The non-Newtonian viscous behaviour has been represented by Herschel Bulkley model. Non-uniform cross-sectional nature of the arteriole and venule have been emphasized in the study in the study. However, arteriole and venule have been assumed to be axisymmetric and the flow that take place through it has also been considered axi-symmetric.

We take  $(R, \theta, Z)$  as the cylindrical coordinates of the location of a fluid particle,  $R$  being the

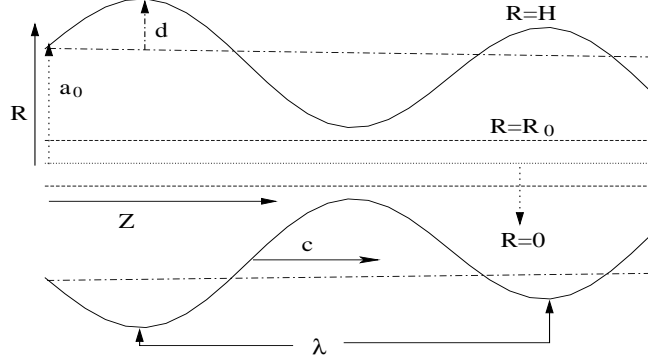


Fig. 1 : A physical sketch of the problem

radius of the tube.  $Z$  is measured in the direction of wave propagation. Let  $R = H$  (cf. Fig. 1) represent the wall of arteriole or venule that is considered to be induced by a progressive sinusoidal, SSD expansion or contraction wave train respectively propagating with a constant speed  $c$  travelling down the wall, such that

$$H = a(Z) + b \sin\left(\frac{2\pi}{\lambda}(Z - ct_1)\right), \quad (1)$$

$$H = \begin{cases} a(Z) + b \sin\left(\frac{\pi}{\lambda_{c1}}(Z - ct_1)\right) & : \text{ if } 0 \leq Z \leq \lambda_{c1} \\ a(Z) & : \text{ if } \lambda_{c1} \leq Z \leq \lambda, \end{cases} \quad (2)$$

$$H = \begin{cases} a(Z) - b \sin\left(\frac{\pi}{\lambda_{c1}}(Z - ct_1)\right) & : \text{ if } 0 \leq Z \leq \lambda_{c1} \\ a(Z) & : \text{ if } \lambda_{c1} \leq Z \leq \lambda; \end{cases} \quad (3)$$

with  $a(Z) = a_0 + k_1 Z$  where  $a(Z)$  represents the radius of the arteriole or venule at any axial distance  $Z$  from inlet,  $a_0$  being the radius at the inlet,  $k_1 (< 1)$  a constant whose magnitude depends on the length of the arteriole or venule as well as on the inlet and exit dimensions,  $b$  the wave amplitude,  $t_1$  the time and  $\lambda$  the wave length. The SSD expansion/contraction wave defined by equations (2) and (3) means that these waves are confined to a portion of length  $\lambda_{c1}$ .

### 3. Analysis

With the consideration made above, the motion of blood in the arteriole or venule can be assumed to be governed by the partial differential field equations

$$\nabla \cdot \mathbf{V} = 0 \quad (4)$$

$$\nabla \sigma + \rho f = \rho \frac{d\mathbf{V}}{dt_1}, \quad (5)$$

where  $\mathbf{V}$  is the velocity,  $f$  the body force per unit mass,  $\rho$  the density and  $\frac{d}{dt_1}$  the material time derivative. Further,  $\sigma$  being the Cauchy stress defined by

$$\sigma = -\bar{P}I + T,$$

$$T = 2\mu D + S,$$

$$S = 2\eta D,$$

D being the symmetric part of the velocity gradient,

$$D = \frac{1}{2}[L + L^T], L = \nabla \mathbf{V},$$

$-\bar{P}I$  denotes the indeterminate part of the stress due to the constraint of incompressibility, where  $\mu$  and  $\eta$  represent viscosity parameters. The Herschel-Bulkley model is the representative of the combined effect of Bingham plastic and power-law behavior of the fluid. When strain-rate is low such that  $\dot{\gamma} < \frac{\bar{\tau}_0}{\mu_0}$ , the material acts like a viscous fluid with constant viscosity  $\mu_0$ . But when the strain rate increases and the yield stress threshold,  $\bar{\tau}_0$ , is reached, the fluid behavior is described by a power law of the form

$$\eta = \frac{\bar{\tau}_0 + m \left\{ \dot{\gamma}^n - \left( \frac{\bar{\tau}_0}{\mu_0} \right)^n \right\}}{\dot{\gamma}},$$

where m and n denote respectively the consistency factors and the power law index.  $n < 1$  corresponds to a shear thinning fluid, while for a shear thickening fluid  $n > 1$ . In the case of a uniform tube, if the tube length is an integral multiple of the wavelength and the pressure difference between the ends of the tube is a constant, the flow is steady in the wave frame. Since in the present study, the geometry of wall surface is non-uniform, the flow is inherently unsteady in the laboratory frame as well as in the wave frame of reference. The equations (Herschel and Bulkley 1926) that govern the fluid motion in a micro-vessel :

$$\rho \left( \frac{\partial U}{\partial t} + U \frac{\partial U}{\partial Z} + V \frac{\partial U}{\partial R} \right) = -\frac{\partial P}{\partial Z} + \frac{1}{R} \frac{\partial (R\tau_{RZ})}{\partial R} + \frac{\partial \tau_{ZZ}}{\partial Z} \quad (6)$$

$$\rho \left( \frac{\partial V}{\partial t} + U \frac{\partial V}{\partial Z} + V \frac{\partial V}{\partial R} \right) = -\frac{\partial P}{\partial R} + \frac{1}{R} \frac{\partial (R\tau_{RR})}{\partial R} + \frac{\partial \tau_{RZ}}{\partial Z} \quad (7)$$

$$\text{where, } \tau_{ij} = 2\mu E_{ij} = \mu \left( \frac{\partial u_i}{\partial x_j} + \frac{\partial u_j}{\partial x_i} \right), \quad (8)$$

$$\mu = \begin{cases} \mu_0 & : \text{ for } \Pi \leq \Pi_0, \\ \alpha \Pi^{n-1} + \tau_0 \Pi^{-1} & : \text{ for } \Pi \geq \Pi_0 \end{cases} \quad (9)$$

$$\Pi = \sqrt{2E_{ij}E^{i,j}} \quad (10)$$

The following non-dimensional variables will be introduced in the analysis that follows:

$$z = \frac{Z}{\lambda}, \quad r = \frac{R}{a_0}, \quad u = \frac{U}{c}, \quad v = \frac{V}{c\delta}, \quad \delta = \frac{a_0}{\lambda}, \quad p = \frac{a_0^{n+1}\bar{P}}{\mu c^n \lambda}, \quad t = \frac{ct_1}{\lambda}, \quad h = \frac{H}{a_0}, \quad \phi = \frac{b}{a_0}, \quad q = \frac{\bar{Q}}{a_0 c},$$

$$\lambda_c = \frac{\lambda_{c1}}{\lambda}, \quad \tau_0 = \frac{\bar{\tau}_0}{\mu \left( \frac{c}{a_0} \right)^n}, \quad \tau_{rz} = \frac{\bar{\tau}_{rz}}{\mu \left( \frac{c}{a_0} \right)^n}, \quad \psi = \frac{\Psi}{a_0 c} \quad (11)$$

The equation governing the flow of the fluid can now be written in the form

$$R\delta \left( \frac{\partial U}{\partial t} + U \frac{\partial U}{\partial Z} + V \frac{\partial U}{\partial R} \right) = -\frac{\partial P}{\partial Z} + \frac{1}{R} \frac{\partial \left( \Phi \left( R \frac{\partial U}{\partial R} + R\delta^2 \frac{\partial V}{\partial Z} \right) \right)}{\partial R} + 2\delta^2 \frac{\partial \left( \Phi \frac{\partial U}{\partial Z} \right)}{\partial Z} \quad (12)$$

$$R\delta^3 \left( \frac{\partial V}{\partial t} + U \frac{\partial V}{\partial Z} + V \frac{\partial V}{\partial R} \right) = -\frac{\partial P}{\partial R} + \delta^2 \frac{1}{R} \frac{\partial(R\Phi \frac{\partial V}{\partial R})}{\partial R} + \delta^2 \frac{\partial \left( \Phi \left( \frac{\partial U}{\partial R} + \delta^2 \frac{\partial V}{\partial Z} \right) \right)}{\partial Z} \quad (13)$$

$$\text{where } \Phi = \left| \sqrt{2\delta^2 \left\{ \left( \frac{\partial V}{\partial R} \right)^2 + \left( \frac{V}{R} \right)^2 + \left( \frac{\partial U}{\partial Z} \right)^2 \right\} + \left( \frac{\partial U}{\partial R} + \delta^2 \frac{\partial V}{\partial Z} \right)^2} \right|^{n-1} \\ + \tau_0 \left| \sqrt{2\delta^2 \left\{ \left( \frac{\partial V}{\partial R} \right)^2 + \left( \frac{V}{R} \right)^2 + \left( \frac{\partial U}{\partial Z} \right)^2 \right\} + \left( \frac{\partial U}{\partial R} + \delta^2 \frac{\partial V}{\partial Z} \right)^2} \right|^{-1} \quad (14)$$

With the use of the long wavelength approximation (i.e for small  $\delta$ ) and the lubrication approach (Shapiro *et al* 1969, Srivastava and Srivastava 1984, Mishra and Rao 2005, Usha and Rao 1995, Srivastava and Srivastava 1985), the governing equations stated earlier and the boundary conditions describing the flow in the laboratory frame of reference in terms of the dimensionless variables when  $f=0$  may be rewritten as

$$0 = -\frac{\partial P}{\partial Z} + \frac{1}{R} \frac{\partial(R \frac{\partial U}{\partial R} |\frac{\partial U}{\partial R}|^{n-1} + \tau_0)}{\partial R} \quad (15)$$

$$0 = -\frac{\partial P}{\partial R} \quad (16)$$

$$\psi = 0, \quad \frac{\partial u}{\partial r} = \frac{\partial \left( \frac{1}{r} \frac{\partial \psi}{\partial r} \right)}{\partial r} = 0, \quad \tau_{rz} = 0 \text{ at } r = 0; \quad (17)$$

$$u = \frac{1}{r} \frac{\partial \psi}{\partial r} = 0 \text{ at } r = h \quad (18)$$

The solution of equation (15) subject to the conditions (17) and (18) is given by

$$u(r, z, t) = \frac{1}{(k+1)P} \left[ (Ph - \tau_0)^{k+1} - (Pr - \tau_0)^{k+1} \right], \quad 0 \leq r \leq h \quad (19)$$

where  $P = -\frac{\partial p}{\partial z}$ ,  $k = \frac{1}{n}$ .

If  $r_0$  be the radius of plug flow region,

$$\frac{\partial u}{\partial r} = 0 \text{ at } r = r_0,$$

$$\text{so that } r_0 = \tau_0/P.$$

If  $\tau_{rz} = \tau_h$  at  $r=h$ , we find  $h = \tau_h/P$ .

$$\text{Thus } \frac{r_0}{h} = \frac{\tau_0}{\tau_h} = \tau \text{ (say), } 0 < \tau < 1 \quad (20)$$

Then we find the plug velocity as

$$u_p = \frac{(Ph - \tau_0)^{k+1}}{(k+1)P} \quad (21)$$

In order to determine the stream function, we use the boundary conditions

$$\psi_p = 0 \text{ at } r = 0$$

and  $\psi = \psi_p$  at  $r = r_0$ .

Integrating (19) and (21), the stream function is found in the form

$$\psi = \frac{P^k}{k+1} \left[ \frac{r^2}{2} (h-r_0)^{k+1} - \frac{(r-\tau_0)^{k+2}}{k+2} \right], \quad r_0 \leq r \leq h \quad (22)$$

$$\text{and } \psi_p = \frac{P^k (h-r_0)^{k+1} r^2}{2(k+1)}, \quad 0 \leq r \leq r_0 \quad (23)$$

The instantaneous rate of volume flow through the tube,  $\bar{Q}$ , is given by

$$\begin{aligned} \bar{Q}(z, t) &= 2 \int_0^{r_0} r u dr + 2 \int_{r_0}^h r u dr \\ &= \frac{P^k (h-r_0)^{k+1} (h^2 (k^2 + 3k + 2) + 2r_0 h (k+2) + 2r_0^2)}{(k+1)(k+2)(k+3)}, \quad k = \frac{1}{n} \end{aligned} \quad (24)$$

$$\begin{aligned} \text{Now } \frac{\partial p}{\partial z} &= - \left[ \frac{\bar{Q}(z, t) (k+1)(k+2)(k+3)}{(h-r_0)^{k+1} (h^2 (k^2 + 3k + 2) + 2r_0 h (k+2) + 2r_0^2)} \right]^n \\ &= - \left[ \frac{\bar{Q}(z, t) (k+1)(k+2)(k+3)}{h^{k+3} (1-\tau)^{k+1} ((k^2 + 3k + 2) + 2\tau(k+1) + 2\tau^2)} \right]^n \end{aligned} \quad (25)$$

The average pressure rise per wave length is calculated as

$$\Delta p = - \int_0^1 \int_0^1 \left( \frac{\partial p}{\partial z} \right) dz dt \quad (26)$$

One may observe that when  $n = 1$ ,  $\tau = 0$  and  $k_1 = 0$ , the equations (19), (22), (24) and (25); the expressions exactly reduce to those obtained by Shapiro *et al* (1969). Our results also match with those of Lardner and Shack (1972), when the eccentricity of the elliptical motion of cilia tips is set equal to zero in their analysis for a Newtonian fluid flowing on a uniform channel. If we put  $n = 1$  and  $r_0 = 0$ , equation (18) tallies with that obtained by Gupta and Seshadri (1976) for a Newtonian fluid of constant viscosity.

#### 4. Quantitative Study

Theoretical estimates of different physical quantities that are of relevance to the physiological problem of blood flow in the micro-circulatory system have been obtained on the basis of the present study. For this purpose, the following valid data that are valid in the physiological range (Guyton and Hall 2006, Srivastava and Srivastava 1984, Fung 1981, Barbee *et al* 1994) have been used:

$a_0 = 10$  to  $60 \mu m$ ,  $\phi = 0.1$  to  $0.9$ ,  $\frac{a_0}{\lambda} = 0.01$  to  $0.02$ ,  $\Delta p = -300$  to  $50$ ;  $\tau = 0.0$  to  $0.2$ ;  $Q=0$  to  $2$ ,  $n = \frac{1}{3}$  to  $2$ . The value of  $k_1$  that is considered with the non-uniform geometry of the micro-vessel, the value of  $k_1$  here has been chosen to match with physiological system. Thus for arterioles, which are of converging type, the width of the outlet of one wave length is 25% less than that of inlet, while in the case of diverging tubes (e.g. venules), the width



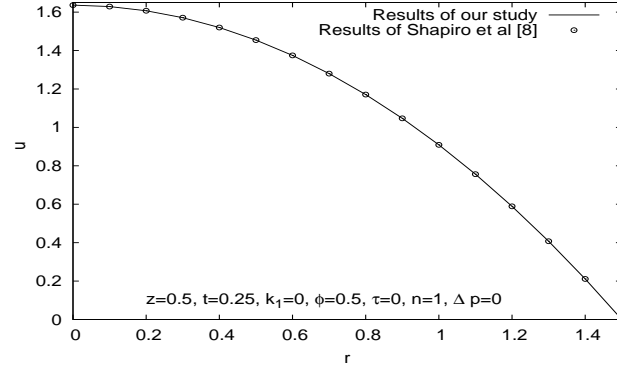
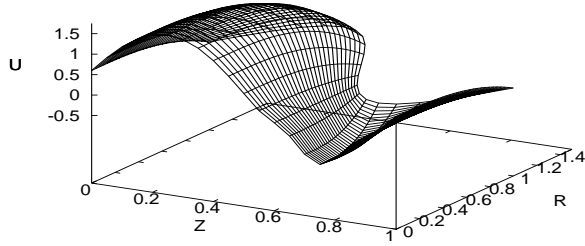
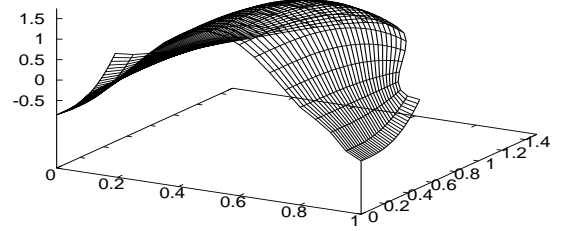


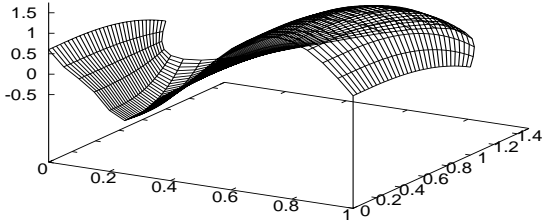
Fig. 2: Variation of axial velocity in the radial direction at  $Z=0.5$



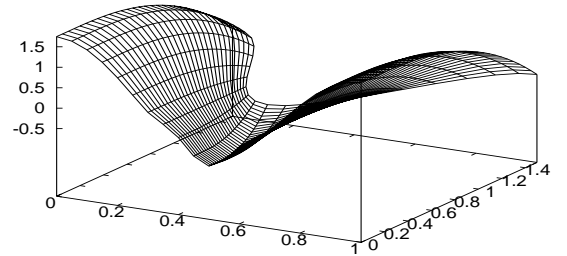
(a)



(b)



(c)



(d)

Figs. 3 : Aerial view of the velocity distribution at different instants,  $n = 2/3$ ,  $k_1 = 0$ ,  $\Delta p = 0$ ,  $\tau = 0.1$ ,  $\phi = 0.5$  for a non-Newtonian fluid of shear thinning type (a)  $t=0.0$  (b)  $t=0.25$  (c)  $t=0.5$  (d)  $t=0.75$ .

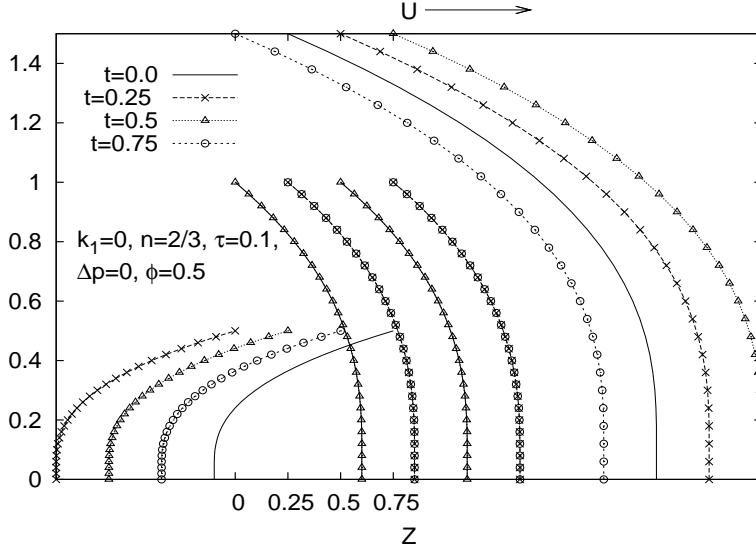


Fig. 4 : Velocity distribution at different instants of time(cf. Fig. 6 of [?])

of the outlet of one wave length is 25% more than that of inlet. To obtain the quantitative results, the instantaneous rate of volume flow  $\bar{Q}(z, t)$  has been considered to be periodic in  $(z-t)$  (Srivastava and Srivastava 1984, Gupta and Seshadri 1976, Srivastava and Srivastava 1983), so that  $\bar{Q}$  appearing in equation (13) can be represented as

$$\bar{Q}^n(z, t) = \begin{cases} Q^n + h^2 - 1 - \phi^2/2 & : \text{for sinusoidal wave,} \\ Q^n + h^2 - 1 - \lambda_c \phi^2/2 - 4\lambda_c \phi/\pi & : \text{for SSD expansion wave;} \\ Q^n + h^2 - 1 - \lambda_c \phi^2/2 + 4\lambda_c \phi/\pi & : \text{for SSD contraction wave;} \end{cases} \quad (27)$$

$Q$  being the time-averaged flow flux. Since the right hand side of equation (13) cannot be integrated in closed form, for non-uniform/uniform geometry, for further investigation of the problem under consideration, we had to resort to the use of software Mathematica. This helped us to calculate the numerical estimate of the pressure rise,  $\Delta p$ .

#### 4.1. Distribution of Velocity

For different values of the amplitude ratio  $\phi$ , flow index number  $n$ ,  $k_1$  and  $\tau$ , Figs. 2-6 present the distribution of axial velocity in the cases of free pumping, pumping and co-pumping zones. It has been shown in Fig. 2 that the results computed on the basis of our study for the particular case of a Newtonian fluid tally well with the results reported by Shapiro *et al* (1969) when the amplitude ratio  $\phi = 0.5$ . Since the velocity profiles along with the radius of the tube change with time, we have investigated the distribution of velocity at a time an interval of a quarter of a wave period. Figs. 3 gives us the aerial view of a few typical axial velocity distribution for a Newtonian fluid and a shear-thinning fluid ( $n=2/3$ ) flowing in uniform micro-vessels, while Fig. 4 (cf. Fig. 6 of Takabatake and Ayukawa 1982) shows the velocity distribution in a vessel.

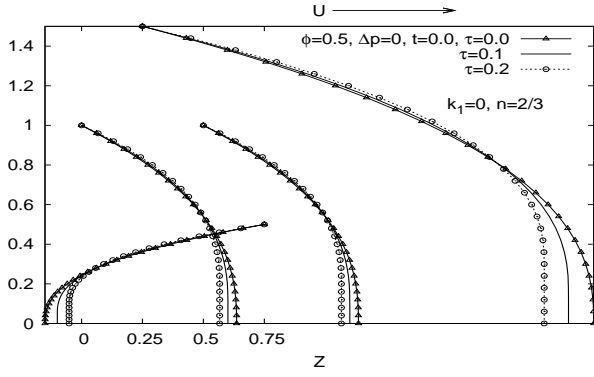
Figs. 5 reveals that at any instant of time, there exists a retrograde flow region. However, the forward flow region is here predominant since the time averaged flow rate is positive. For a shear-thinning fluid ( $n=2/3$ ), the present study indicates that there exist two stagnation points on the axis. For example, at time  $t=0.25$ , one of the stagnation points lies between  $Z=0.0$  and  $Z=0.25$ , while the other lies between  $Z=0.75$  and  $Z=1.0$ . Similar observations were made numerically by Takabatake and Ayukawa (1982) for a Newtonian fluid. Figs. 5(a)-(b) depict that in both the regions, as  $\tau$  increases, the magnitude of velocity decreases for both types of fluids. It can be observed from Fig. 5(c) that for a Herschel-Bulkley fluid ( $n=2/3$ ) with  $\Delta p = 0$ , the velocity in both the regions of backward and forward flows is enhanced as the value of  $\phi$  increases when  $0 < \phi < 0.6$ , but beyond  $\phi = 0.6$ , the velocity in the backward flow region decreases with  $\phi$  increasing.

It is worthwhile to observe the significant influence of the rheological fluid index 'n' on the velocity distribution (cf. Figs 5(d)-(i)) for flows in uniform/non-uniform vessels. Figs. 5(d)-(i) reveal that the parabolic nature of the velocity profiles is disturbed due to non-Newtonian effect. Magnitude of the velocity decreases at the maximum occlusion region; while in the remaining regions including backward flow region, a reverse trend is noticed with an increase in the value of 'n' (cf Figs. 5(d-f, h-i)). However, in a diverging tube, flow reversal is seen to vanish for shear thickening fluids satisfying the rheological fluid index ' $n > 3/2$ ' (cf. Fig. 5(g)). The last two observations (cf. Figs. (c,g)) are in contrast to the case of two dimensional channel flow was. For a converging vessel, the magnitude of the velocity is greater than that of a uniform vessel; however, for a diverging vessel, our observation is altogether different. It is essential to mention that Figs. 5(j)-(l) show the influence of pressure on velocity distribution for shear thinning /shear thickening fluids. In the case of a uniform/diverging vessel, if  $\Delta p$  decreases, the flow reversal tends to decrease; however for a converging tube, although there is reduction in the region of flow reversal, the change is not significant for shear thickening fluid. It is important to mention that flow reversal due to change in sign of the vorticity or the shear stress along the wavy wall.

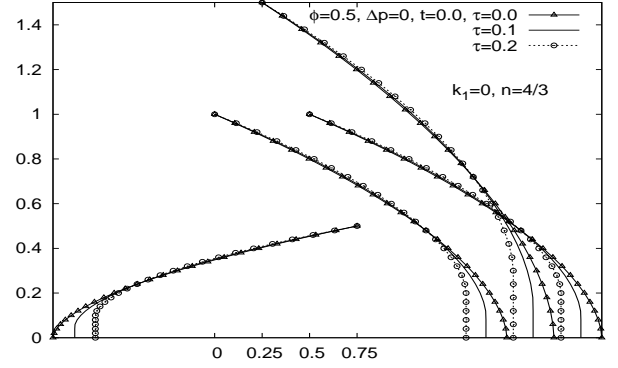
The results corresponding to SSD wave is shown in Figs. 5(m-n). It is seen that for SSD expansion waves, there is no backward flow and its magnitude is considerable less as compared to the sinusoidal wave (cf. Fig. 4). Moreover, as  $\lambda_c$  increases, velocity is seen to rise except near around  $Z=0.25$  where it decreases if  $\lambda_c$  exceeds 0.6. While for SSD contraction waves, Fig. 5(n) shows that if  $\lambda_c = 0.2$ , there is no backward flow within one wave length. If  $\lambda_c > 0.3$ , backward flow is observed from  $Z=0.15$  to  $Z=0.7$ .

#### 4.2. Pumping Behaviour

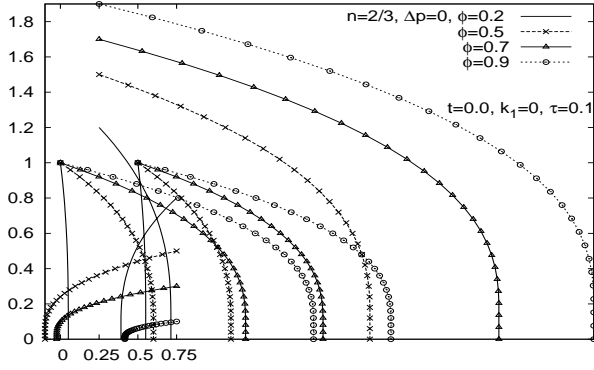
Figs. 6 give the variation of volumetric flow rate of peristaltic waves in the case of our present study for different values of the amplitude ratio  $\phi$ , flow index number  $n$ ,  $\tau$ ,  $k_1$ . Shapiro et al. [?] used lubrication theory to show that the flow rate averaged over one wave varies linearly with the pressure difference. For our study of the peristaltic transport of a non-Newtonian fluid, the



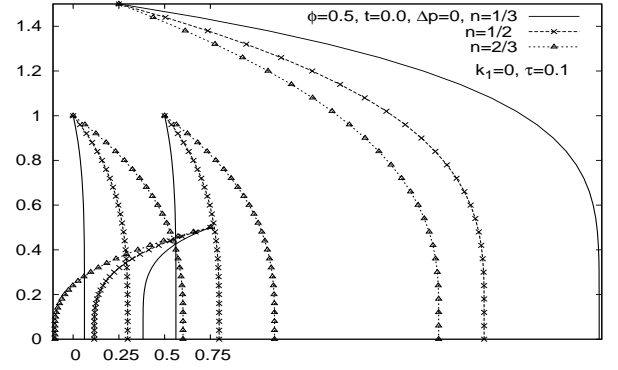
(a)



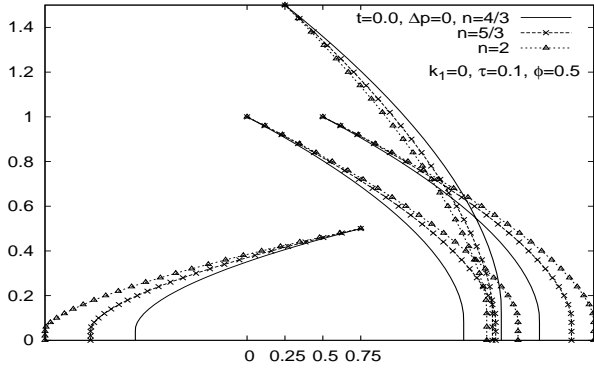
(b)



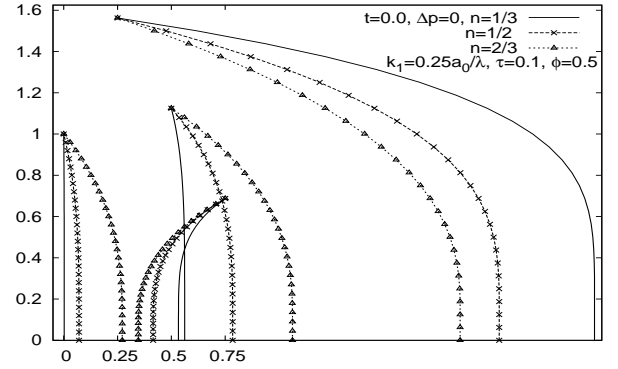
(c)



(d)

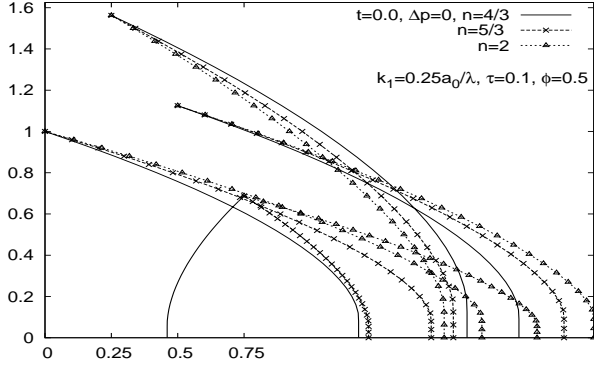


(e)

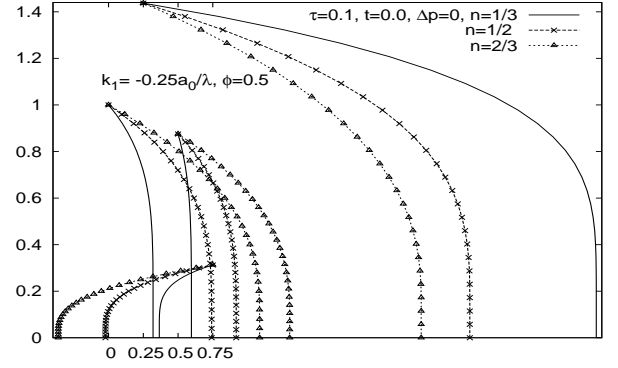


(f)

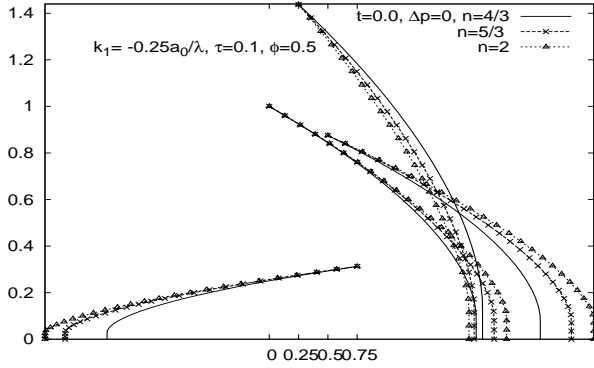
relationship between the pressure difference and the mean flow rate is found to be non-linear (cf. Figs 6). Figs. 6 show that for a non-Newtonian fluid, the mean flow rate,  $Q$  increases as  $\Delta p$  decreases. Plots in Figs. 6(a) and (b) indicate that the pumping region enhances with an increase in the value of the amplitude ratio,  $\phi$  for both shear thinning and shear thickening fluids. It has been illustrated in Figs. 6(c-e) that the influence of the rheological parameter 'n' on the pumping performance in uniform/diverging/converging vessels that the pumping region ( $\Delta p > 0$ ) significantly enhances with the increase in the value of 'n', while in the co-pumping



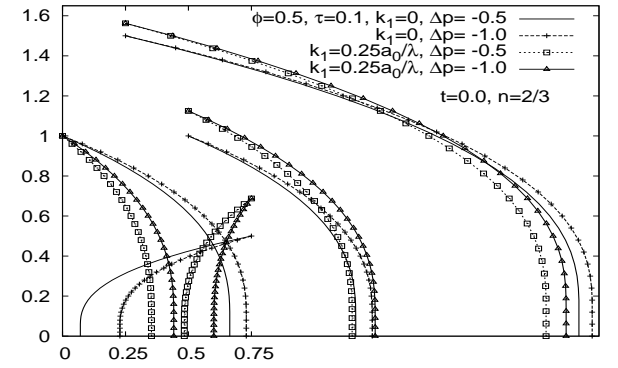
(g)



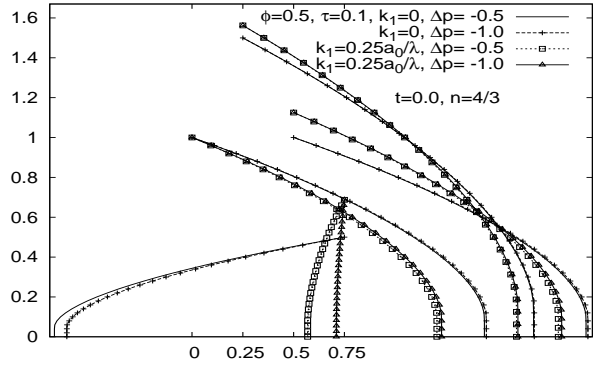
(h)



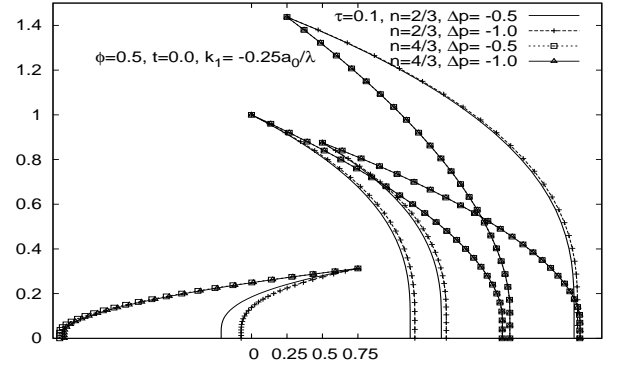
(i)



(j)



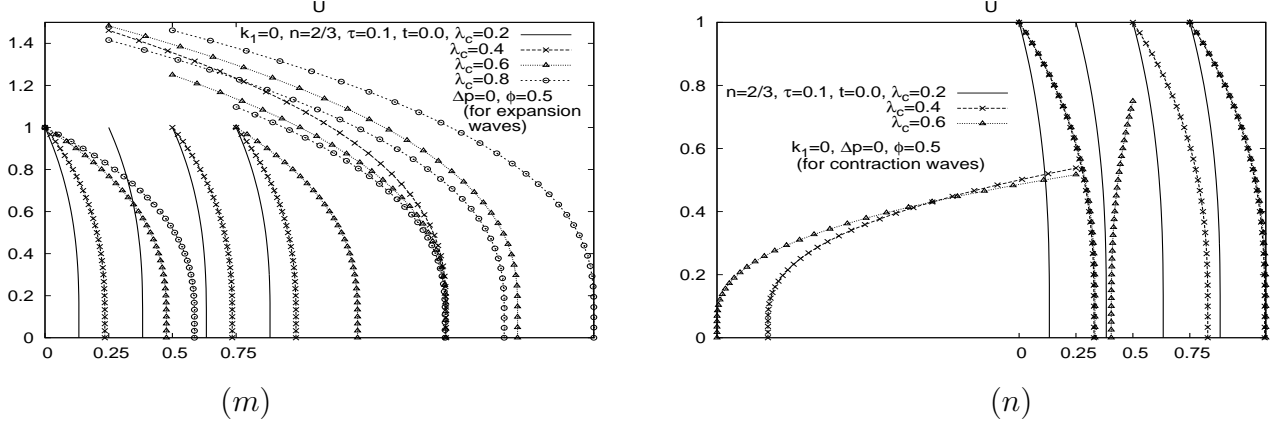
(k)



(l)

region ( $\Delta p < 0$ ) the pressure-rise decreases when  $Q$  exceeds a certain value. As seen in Figs. 6(f-g),  $Q$  is not significantly affected by the value of the parameter  $\tau$  for free pumping case. We further find that for both shear-thinning and shear thickening fluids, pumping region increases with  $\tau$  increasing. Moreover, when  $Q$  exceeds a certain critical limit,  $\Delta p = 0$ , pressure rise decreases with the increase in  $\tau$ .

The effect of SSD wave on pumping is revealed in Figs. 6(h-i). Unlike sinusoidal wave form  $Q$  increases significantly in pumping, free-pumping as well as co-pumping regions for SSD



Figs. 5: Distribution of velocity in different situations

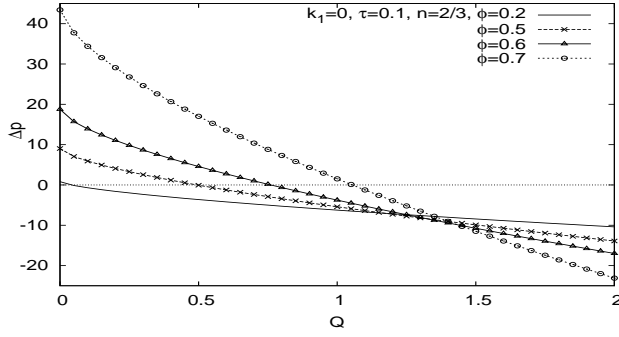
expansion wave fronts as  $\lambda_c$  increases. For SSD contraction wave fronts, our observation is altogether different against SSD expansion wave fronts. However,  $Q \leq 0$  when  $\Delta p < 0$  for shear-thinning fluids in the case of contraction waves. This observation is in contrast to the case of sinusoidal was.

#### 4.3. Streamlines and Trapping

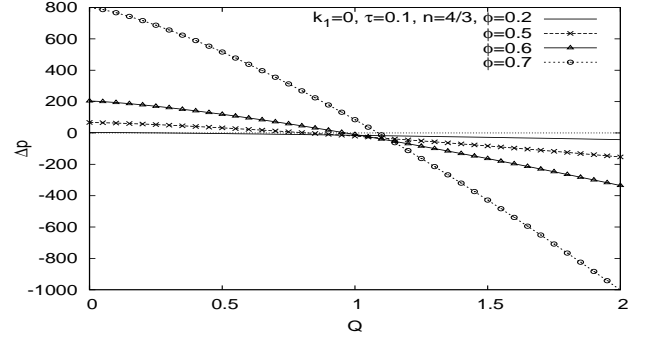
It is known that one of the important characteristics of peristaltic transport is the phenomenon of trapping . It occurs under some conditions as streamlines on the central line are split to enclose a bolus of fluid particles circulating along closed streamlines in the wave frame of reference. Then the trapped bolus moves with a speed equal to that of the wave. This physical phenomenon may have responsibility to the formation of thrombus in blood. Under the purview of the present study, Fig. 7-10 give an insight into the changes in the pattern of streamlines and trapping that occur due to the changes in the values of different parameters that govern the flow of blood in the wave frame of reference. Figs. 7 provide the streamline patterns and trapping of a shear-thinning fluid for different values of  $\phi$ . With an increase in  $\phi$ , the bolus is found to appear in a distinct manner. Streamlines for different fluid indices 'n' are depicted in Figs. 8. These figures indicate that occurrence of trapping is strongly influenced by the value of the fluid index. Figs. 9 show that trapped bolus increases in size and also that it has a tendency to move towards the boundary as the flow rate increases. It is important to note that the bolus appearing for  $\tau = 0$  is going to disappears as the value of  $\tau$  rises (Figs. 10).

#### 4.4. Distribution of Wall Shear Stress

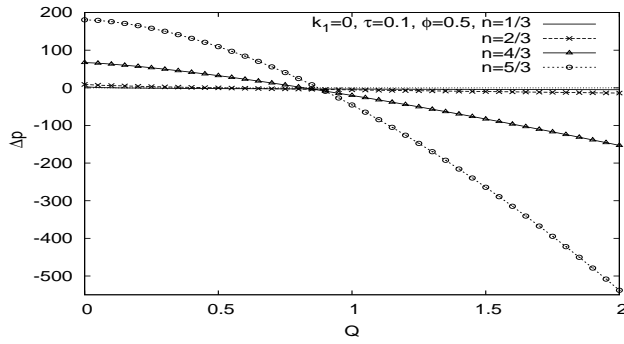
It is known that if the shear stress generated on the wall of a blood vessel exceeds a certain limit, the constituents of blood are likely to be damaged. Also, the magnitude of the wall shear stress has a vital role in the process of molecular convection at high Prandtl or Schmidt number (Higdon 1985). In view of the above observations, it is important to study the shear



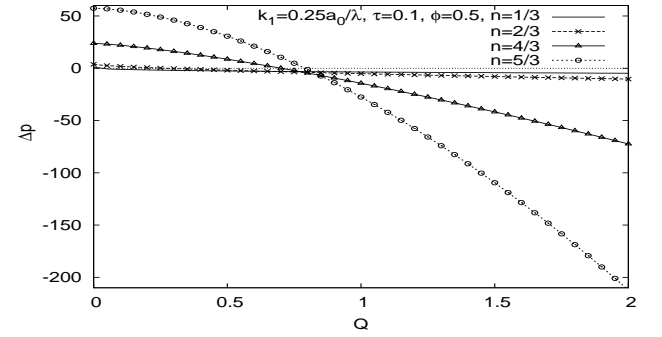
(a)



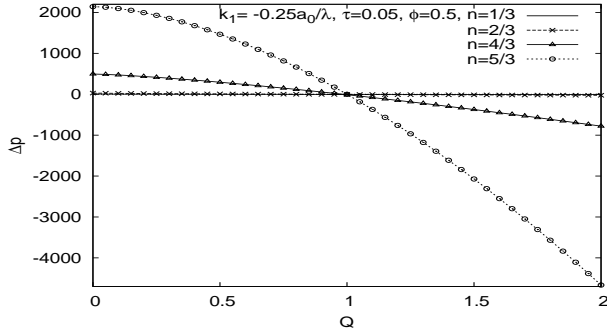
(b)



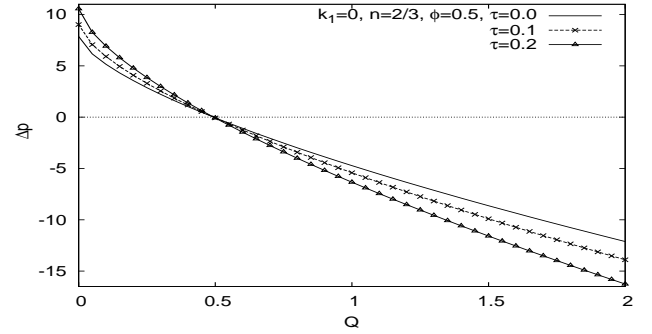
(c)



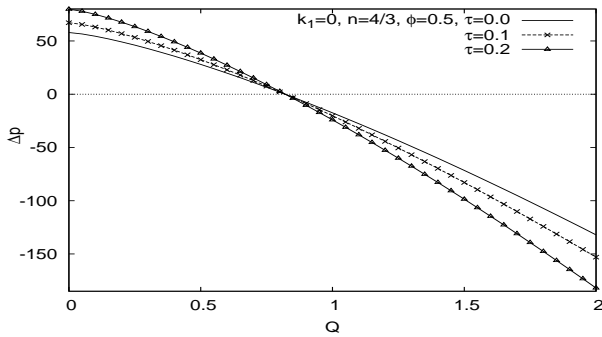
(d)



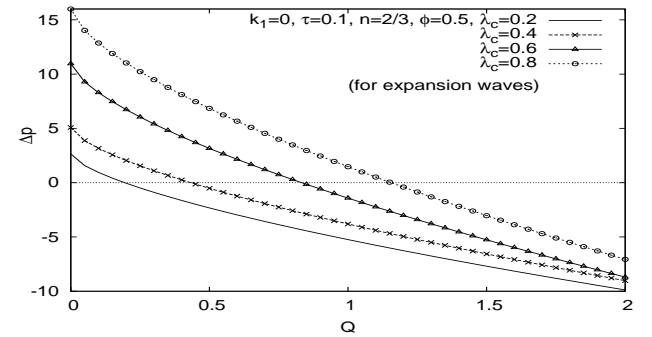
(e)



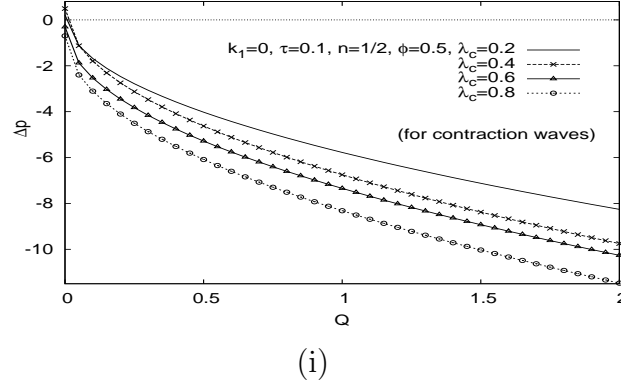
(f)



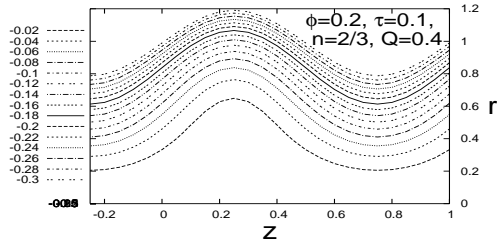
(g)



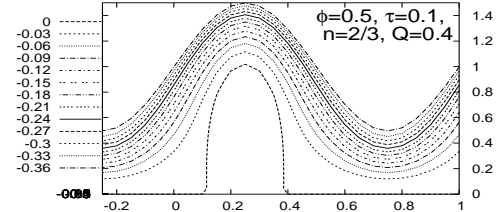
(h)



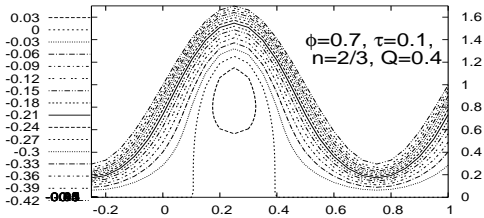
Figs. 6: Pressure rise versus flow rate



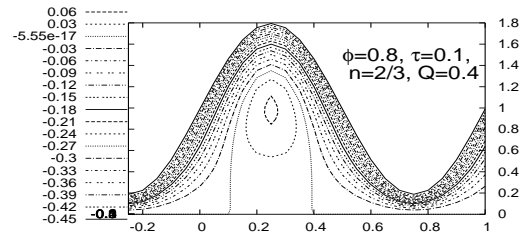
(a)



(b)



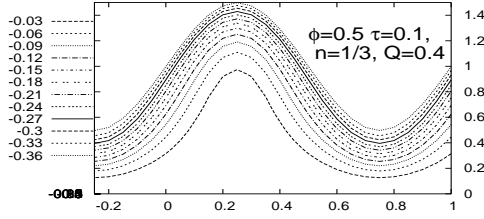
(c)



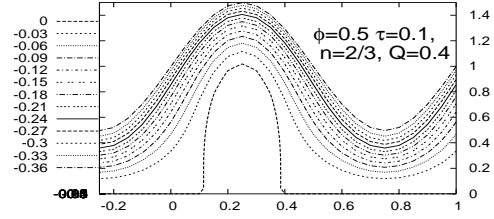
(d)

Figs. 7 : Streamline patterns for peristaltic flow of a shear-thinning fluid for different values of  $\phi$  ( $n=2/3$ ,  $Q = 0.4$ ,  $k_1 = 0$ ,  $\tau = 0$ )

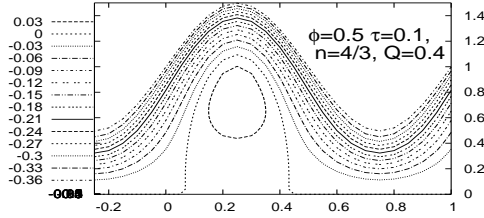




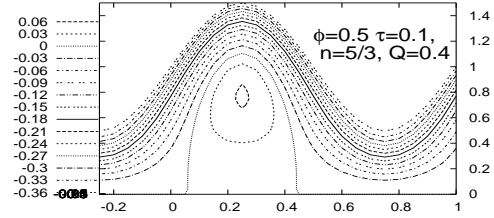
(a)



(b)



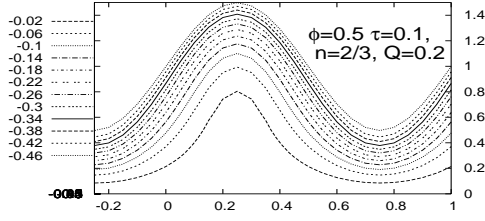
(c)



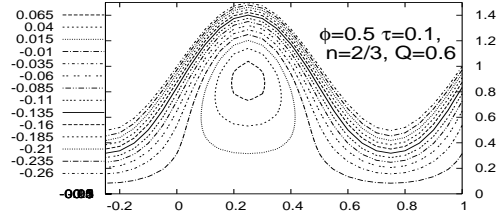
(d)

Figs. 8 : Streamline patterns and trapping in the case of peristaltic flow for different values of physiological fluid index 'n' when  $\phi = 0.5$ ,  $\tau = 0.1$ ,  $k_1 = 0$ ,  $Q = 0.4$

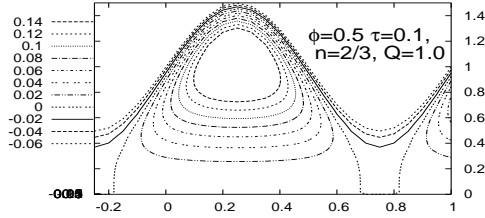
stress that is developed during the hemodynamical flow of blood in arteries. The wall shear stress distributions are plotted in Figs 11 under varied conditions. The distributions of wall shear stress at four time instants during one complete wave period have been presented in Fig. 11(a). It may be observed from this figure that at each of these instants of time, there exist two peaks in the wall shear stress distribution, with a gradual ramp in between; however, negative peak of wall shear stress,  $\tau_{min}$  is not as large as the maximum wall shear stress,  $\tau_{max}$ . The transition from  $\tau_{min}$  to  $\tau_{max}$  of the wall shear takes place in some zone between the minimum and maximum radii of the vessel. At the location where the maximum occlusion occurs, wall shear stress along with the pressure is maximum. Since the pressure gradient to the left of this location takes positive value, the local instantaneous flow will take place towards the left of  $\tau_{max}$ . This may lead to some consequences may be happen, for example, if the shear rate at the crest exceeds some limit, a dissolving wavy wall will have a tendency to level out. Moreover, some bio-chemical reaction between the wall material and the constituents of blood may set in. As a result of this, there may be deposition of the products of the chemical reaction on the endothelium and consequently wall amplitude may increase at a rapid rate. This is likely to lead to clogging of the blood vessel.



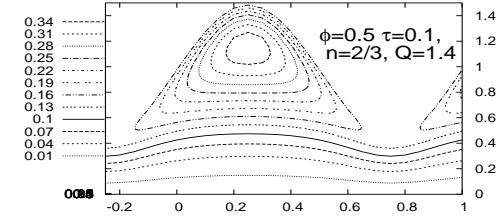
(a)



(b)



(c)

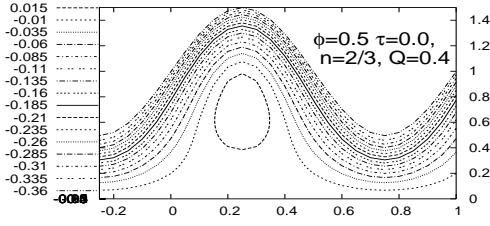


(d)

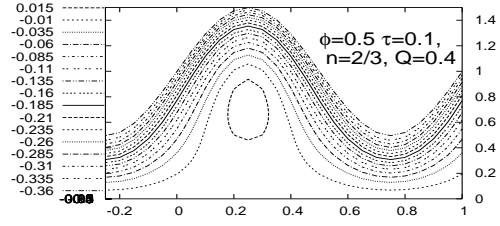
Figs. 9 : Streamline patterns and trapping for the effect of  $Q$  when  $n = 2/3$ ,  $\phi = 0.5$ ,  $k_1 = 0$ ,  $\tau = 0.1$

The peaks of the wall shear stress distribution on both sides of  $\tau_{max}$  are small and hence the local instantaneous flow will occur in the direction of the peristaltic wave. For a Herschel-Bulkley fluid, Figs. 11(b-c) show that in the contracting region where occlusion takes place, there is a remarkable increase in the wall shear stress due to an increase in the value of  $\phi$  for shear-thinning as well as shear-thickening fluids. With the increase in  $\phi$ , magnitude of  $\tau_{min}$  increases in the expanding region for shear-thinning/shear-thickening fluids, although the effect is not very prominent. It may be observed from Fig. 11(d) that  $\tau_{max}$  increases with increase in  $\tau$ , while  $\tau$  has little effect upon  $\tau_{min}$ .

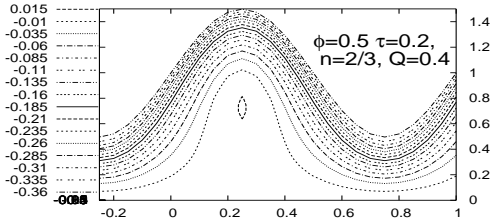
The quantum of influence of the rheological fluid index 'n' on the distribution of wall shear stress is shown in Figs. 11(e-g) for uniform/non-uniform blood vessels. In all types of vessels studied here,  $\tau_{max}$  increases with the increase in 'n'. Moreover, it is very important to mention that the shear stress difference between the outlet and the inlet in the case of a converging vessel is exceedingly large in comparison to the case of a diverging vessel. As the time averaged flow rate increases, Figs. 11(h-j) indicate very clearly that the wall shear stress tends to decrease for all the types of vessel examined here. One can observe from Figs. 11(k-l) that  $\tau_h$  changes its values within the region of SSD wave activation; beyond this, however it remains constant.



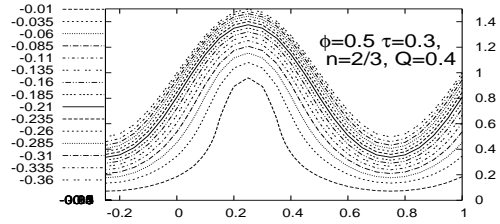
(a)



(b)



(c)

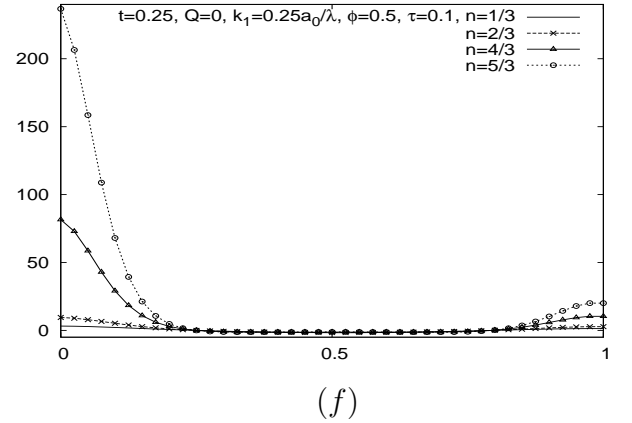
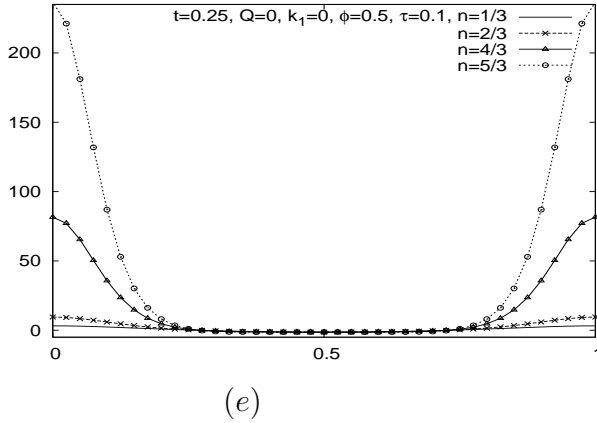
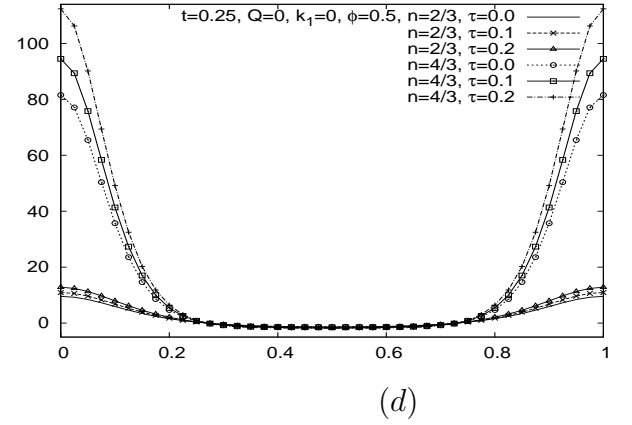
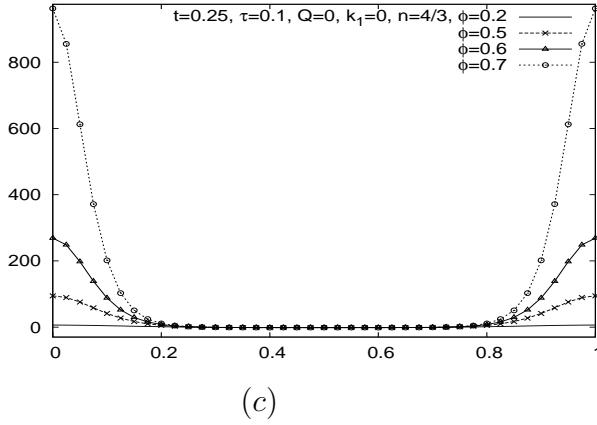
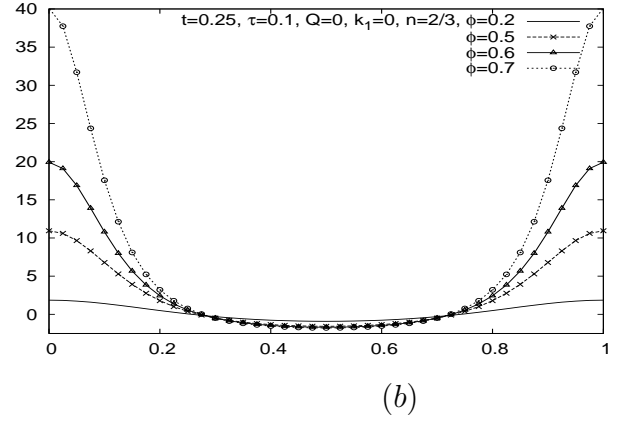
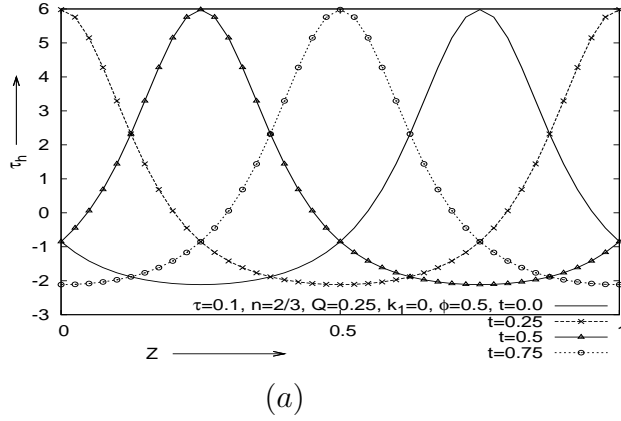


(d)

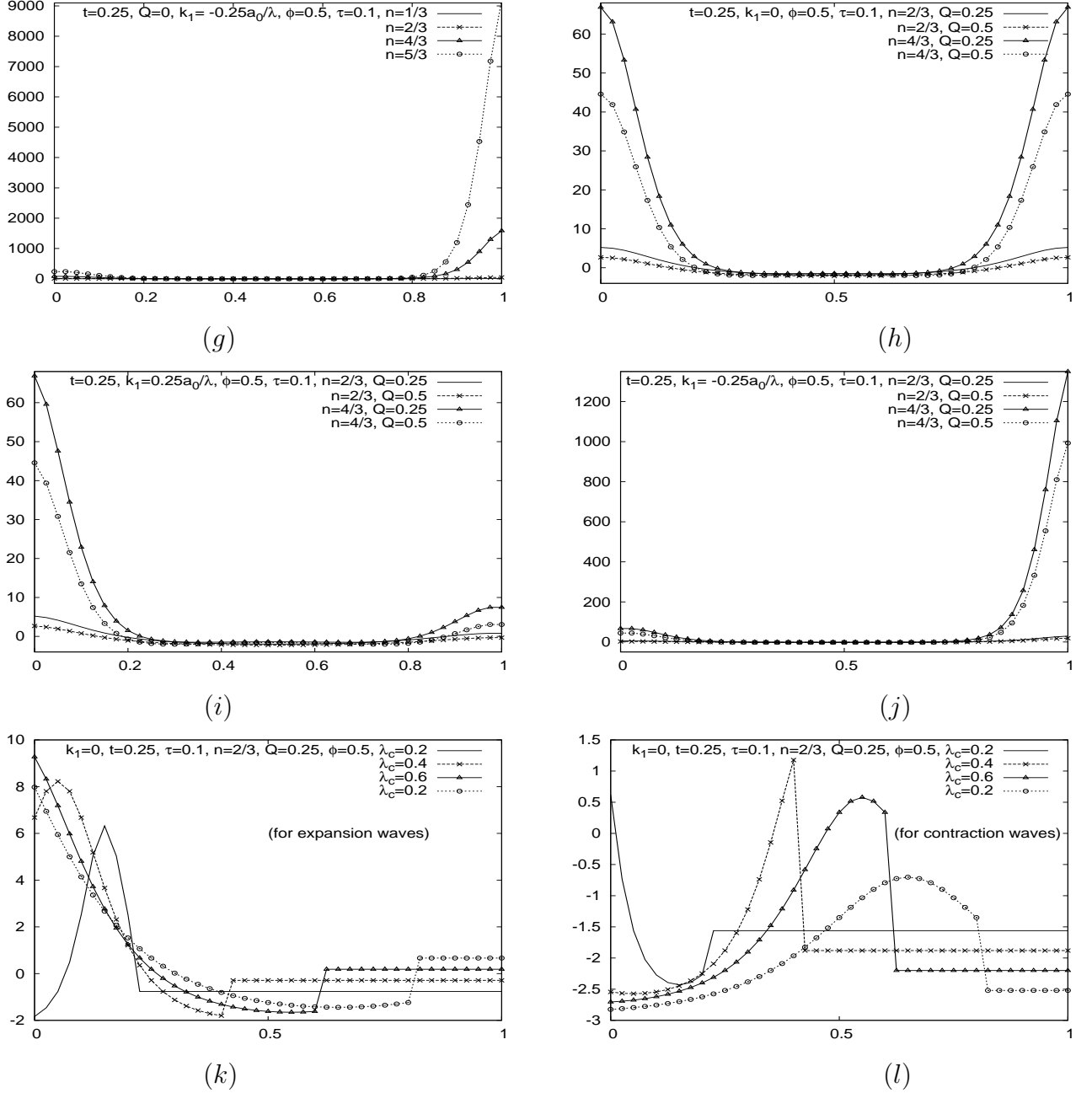
Figs. 10: Streamline patterns for different values of  $\tau$  in the case of peristaltic flow when  $n = 2/3$ ,  $\phi = 0.5$ ,  $k_1 = 0$ ,  $Q = 0.4$

## 5. Summary and Conclusion

The present paper deals with the peristaltic motion of blood in the micro-circulatory system, by taking into account the non-Newtonian nature of blood and the non-uniform geometry of the micro-vessels, e.g. arterioles and venules. The non-Newtonian viscosity of blood is considered to be of Herschel-Bulkley type. The effects of amplitude ratio, mean pressure gradient, yield stress and the rheological fluid index  $n$  on distribution of the velocity and wall shear stress, pumping phenomena, streamline pattern and trapping are investigated under the purview of the lubrication theory. Experimental observations have revealed that in the case of roller pumps, the fluid elements are quite prone to significant damage; also during the process of transportation of fluids in living structures executed by using arthro-pumps, the fluid particles are likely to be appreciably damaged. Qualitative and quantitative studies of the current analysis for the wall shear stresses have a significant bearing in extra-corporeal circulation, where the heart-lung machine is usually used and thereby there is a chance of the erythrocytes of blood being damaged. Thus the present study bears the potential of significant application in biomedical engineering and technology.



The present study reveals that at any instant of time, there is a retrograde flow region for Herschel-Bulkley type of non-Newtonian fluids like blood when  $\Delta p \leq 0$ . The regions of forward/retrograde flow advance at a faster rate, if the values of  $n$  and  $\phi$  are raised. In the case of a uniform/diverging tube, the flow reversal tends to decrease when  $\Delta p$  tends to be negative; however, for a converging tube such an observation is not very prominent. Moreover, the present study shows that non-uniform geometry affects quite significantly the distributions of velocity and the wall shear stress as well as pumping and other flow characteristics. The amplitude ratio  $\phi$  and the rheological index ' $n$ ' are very sensitive parameters in changing the peristaltic pumping



Figs. 11: Wall shear stress distribution in different situations.

characteristics and the distribution of velocity and wall shear stress. Moreover, the parabolic nature of the velocity profiles is found significantly disturbed by rheological fluid index 'n'.

From the present study we may conclude that for SSD expansion waves, the pumping performance is better than that in the case of sinusoidal waves. It is also important to note that the backward flow region is totally absent in the case of SSD expansion waves. Further, it may be concluded that backward flow originates from the contraction of vessels.

**Acknowledgment:** *One of the authors, S.Maiti is thankful to the Council of Scientific and Industrial Research (CSIR), New Delhi for awarding an SRF.*

## References

- Misra J C and Pandey S K 1999 Peristaltic transport of a non-Newtonian fluid with a peripheral layer. *Int. J. Eng. Sci.* **37**, 1841-58
- Misra J C and Pandey S K 2001 Peristaltic flow of a multi layered power-law fluid through a cylindrical tube. *Int. J. Eng. Sci.* **39** 387-402
- Misra J C and Pandey S K 2002 Peristaltic transport of blood in small vessels: study of a mathematical model *Compu. Math. Appl* **43** 1183-93
- Misra J C and Pandey S K 1995 Peristaltic transport in a tapered tube *Math. Compu. Model.* **22**(8) 137-151
- Misra J C and Pandey S K 2001 A mathematical model for oesophageal swallowing of a food bolus *Math. Compu. Model.* **33**(8-9) 997-1009
- Misra J C and Pandey S K 1994 Peristaltic transport of particle-fluid suspension in a cylindrical tube *Compu. Math. Appl* **28**(4) 131-145
- Misra J C, Maiti S and Shit G C 2008 Peristaltic Transport of a Physiological Fluid in an Asymmetric Porous Channel in the Presence of an External Magnetic Field *J. Mech. Medi. Biol.* **8**(4) 507-525
- Maiti S and Misra J C 2011 Peristaltic Flow of a Fluid in a Porous Channel: a Study Having Relevance to Flow of Bile *Int. J. Eng. Sci.* **49** 950-966
- Guyton A C and Hall J E 2006 *Text Book of Medical Physiology* Elsevier: Saunders Co
- Jaffrin M Y and Shapiro A H 1971 Peristaltic pumping *Annu. Rev. Fluid Mech.* **3** 13-36
- Fung Y C and C S Yih 1968 Peristaltic Transport *J. Appl. Mech.* **35** 669-75
- Shapiro A H Jaffrin M Y and Weinberg S L 1969 Peristaltic pumping with long wavelength at low Reynolds number *J. Fluid Mech.* **37** 799-825
- Srivastava L P and Srivastava V P 1984 Peristaltic transport of blood: Casson model: II *J. Biomech.* **17** 821-29
- Tsiklauri D and Beresnev I 2001 Non-Newtonian effects in the peristaltic flow of a Maxwell fluid *Phys. Rev. E* **64** 036303
- Mishra M and Rao A R 2005 Peristaltic transport in a channel with a porous peripheral layer: model of a flow in gastrointestinal tract *J. Biomech.* **38** 779-789
- Yaniv S, Jaffa A J, Eytan O and Elad D 2009 Simulation of embryo transport in a closed uterine cavity model *Euro. J. Obst. Gynecol. Reprodu. Biol.* **144S** S50-S60
- Jimenez-Lozano J, Sen M and Dunn P F 2009. Particle motion in unsteady two-dimensional peristaltic flow with application to the ureter *Phys. Rev. E* **79** 041901
- Usha S and Rao A R 1995 Peristaltic transport of a biofluid in a pipe of elliptic cross section *J. Biomech.* **28**(1) 45-52
- Takabatake S and Ayukawa K 1982 Numerical study of two-dimensional peristaltic flows *J. Fluid Mech.* **122** 439-465
- Jimenez-Lozano J and Sen M 2010 Particle dispersion in two-dimensional peristaltic *Phys. Fluids* **22** 043303
- Bohme G and Friedrich R 1983 Peristaltic transport of viscoelastic liquids *J. Fluid Mech.* **128** 109-122
- Srivastava L M and Srivastava V P 1985 Peristaltic transport of a non-Newtonian fluid: a applications to the vas deferens and small intestine *Anna. Biomed. Eng.* **13** 137-153
- Provost A M and Schwarz W H 1994 A theoretical study of viscous effects in peristaltic pumping *J. Fluid Mech.* **279** 177-195.
- Chakraborty S 2006 Augmentation of peristaltic micro-flows through electro-osmotic mechanisms *J. Phys. D: Appl. Phys.* **39** 5356-5363
- Rand P W, Lacombe E, Hunt H E and Austin W H 1964 Viscosity of normal blood under normothermic and hypothermic conditions *J. Appl. Physio.* **19** 117-122

- Bugliarello G, Kapur C and Hsiao G 1965 *The profile viscosity and other characteristics of blood flow in a non-uniform shear field* Proc IVth International Congress on Rheology, 4, Symp of Biorheol (Ed. Copley A L), 351-370, Interscience, New York
- Chien S, Usami S, Taylor H M, Lundberg J L and Gregerson M T 1966 Effects of hematocrit and plasma proteins on human blood rheology at low shear rates *J. Appl. Physiol.* **21** 81-87
- Charm S E and Kurland G S 1965 Viscometry of human blood for shear rates of 0-100, 000  $\text{sec}^{-1}$  *Nature* **206** 617-629
- Charm S E and Kurland G S 1974 *Blood Flow and Microcirculation* New York: John Wiley
- Merrill F W, Benis A M, Gilliland E R, Sherwood T K and Salzman E W 1965 Pressure flow relations of human blood in hollow fibers at low flow rates *J. Appl. Physiol.* **20** 954-967
- Blair G W S and Spanner D C 1974 *An Introduction to Bioreheology* Elsevier, Amsterdam
- Fung Y C 1981 *Biomechanics, Mechanical Properties of Living Tissues* Springer Verlag, New York
- White F M 1974 *Viscous Fluid Flow* McGraw-Hill, New York
- Xue H 2005 The modified Casson's equation and its application to pipe flows of shear thickening fluid *Acta Mecha. Sinica* **21** 243-248
- Wiedman M P 1963 Dimensions of blood vessels from distributing artery to collecting vein *Circu. Research* **12** 375-381
- Wiederhielm C A 1967 *Analysis of small vessel function, In Physical Bases of Circulatory Transport: Regulation and Exchange, edited by Reeve, E. B. and Guyton, A. C., 313-326* W. B.Saunders, Philadelphia.
- Lee J S and Fung Y C 1971 Flow in nonuniform small blood vessels *Microvas. Research* **3** 272-287
- Gupta B B and Seshadri V J 1976 Peristaltic pumping in non-uniform tubes *J. Biomech.* **9** 105-109
- Srivastava L M and Srivastava V P 1983 Peristaltic transport of a physio-logical fluid, part I: Flow in non-uniform geometry *Biorheol* **20** 153-166
- Malek J, Necas J and Rajagopal K R 2002 Global existence of solutions for fluids with pressure and shear dependent viscosities *Appl. Math. Let.* **15** 961-967
- Herschel W H and Bulkley R 1926 Konsistenzmessungen von Gummi-Benzollösungen *Kolloid Zeitschrift* **39** 291-300.
- Lardner T J and Shack W J 1972 Cilia transport *Bullet. Math. Biol* **34** 325-335
- Barbee K A, Davies P F and Lal R 1994 Shear stress-induced reorganization of the surface topography of living endothelial cells imaged by atomic force microscopy *Circul Research* **74** 163-171
- Higdon J J L 1985 Stokes flow in arbitrary two-dimensional domains: shear flow over ridges and cavities *J. Fluid Mech.* **159** 195-226